RESEARCH PAPER

# Angular reflectance of suspended gold, aluminum and silver nanospheres on a gold film: Effects of concentration and size distribution

**Mustafa M. Aslan · Thomas Wriedt**

**Abstract** In this article, we describe a parametric study of the effects of the size distribution (SD) and the concentration of nanospheres in ethanol on the angular reflectance. Calculations are based on an effective medium approach in which the effective dielectric constant of the mixture is obtained using the Maxwell–Garnett formula. The detectable size limits of gold, aluminum, and silver nanospheres on a 50-nm-thick gold film are calculated to investigate the sensitivity of the reflectance to the SD and the concentration of the nanospheres. The following assumptions are made: (1) the total number of particles in the unit volume of suspension is constant, (2) the nanospheres in the suspension on a gold film have a SD with three different concentrations, and (3) there is no agglomeration and the particles have a log-normal SD, where the effective diameter, $d_{eff}$ and the effective variance, $v_{eff}$ are given. The dependence of the reflectance on the $d_{eff}$, $v_{eff}$, and the width of the SD are also investigated numerically. The angular variation of the reflectance as a function of the incident angle shows a strong dependence on the effective size of the metallic nanospheres. The results confirm that the size of the nanospheres ($d_{eff}$ <100 nm) can be detected by reflected light from the bottom surface of a gold film with a reasonable sensitivity if a proper angle of incidence is chosen based on the type of metallic particles on a gold thin film at $\lambda = 632$ nm. We show that the optimum incident angle to characterize the size of nanospheres on a gold film is between 70° and 75° for a given concentration with a particular SD.

**Keywords** Angular reflectance · Surface plasmon (SP) · Nanospheres · Size distribution · Effective medium · Gold (Au) · Aluminum (Al) · Silver (Ag) · Nanostructured thin layers

M. M. Aslan (✉)
Materials Institute, TUBITAK Marmara Research Center, 41470 Gebze-Kocaeli, Turkey
e-mail: mustafa.aslan@mam.gov.tr

T. Wriedt
Institut für Werkstofftechnik, Badgasteiner Str. 3, 28359 Bremen, Germany

## Introduction

Nanomaterials and nanoparticles are now being used in a wide range of applications and have become the centrepieces of many new and exciting engineering applications. Their specialized usages are derived from their small size, which allows unique physical, mechanical, electronic, magnetic, optical, and chemical properties that differ from those of the same materials when used in bulk quantities (Feldheim and Foss 2002; Kreibig and Vollmer 1995). For instance, the increased surface area of nanoparticles leads to

increased catalytic activity, improved strength of sintered products, and increased sensitivity for sensor materials (Brune et al. 1998; Shipway et al. 2000). Color pigments and coatings gain additional hiding power and strength with decreasing particle size. Electronic and electromagnetic components have improved mechanical properties and process uniformity (Bohren and Huffman 1983; Kruis et al. 1998), which will most likely benefit the semiconductor industry as finer abrasive materials are developed for polishing silicon wafers, integrated circuits, and recording media. Accordingly, more companies are becoming involved in metallic nanoparticles, either as a strategic technology or as the continuing development of existing products. Inherent to these new applications, there is a keen interest in monitoring particle size to tightly control the nanoparticles' manufacturing processes (Brune et al.1998), and rightly so, as the nano-size of particles may range from 100 nm down to 1 nm, with some size distribution (SD).

Traditional optical monitoring techniques (such as scattering/absorption) may not be sensitive to particle sizes smaller than $\lambda/(2 \times NA)$, where $NA$ is the Numerical Aperture of the optical system and $\lambda$ is wavelength of the light employed. For most optical systems, the $NA$ is less than 1 (unity), which limits the sensitivity to the order of $\lambda/2$, if no other mechanism is involved. Considering that the shortest wavelength in the visible spectrum is about 400 nm, the resolution is usually limited to about 200 nm. Even though both dynamic light scattering (DLS) and static light scattering (SLS) remain the standard approaches for characterization of micron size particles/colloids (Bohren and Huffman 1983; Kerker 1969; Berne and Pecora 1976; Wriedt 2009), the most common characterization methods for nanoparticles are X-ray, SEM, TEM, and AFM, but they are expensive and are not practical for in situ measurements.

Surface plasmons (SPs) can be used in engineering diagnostic applications to monitor physical and chemical changes that affect either the refractive index or the absorption characteristics of the medium (Hutter and Fendler 2004). An SP wave is an electromagnetic wave propagating along the interface between two media, one of them having a negative dielectric constant. The fundamentals of SP waves are well described in the literature (Raether 1988) and

are relatively well understood. SP response of a medium is sensitive to both the refractive index of the medium and the absorption characteristics of the medium (Kolomenskii et al. 2000). One of the advantages of the SP wave is that the incident wave does not propagate through the medium of interest, minimizing the possibility of unrelated light absorption and scattering. Also, SP scattering from metal nanoparticles strongly depends on particle size (Lyon et al. 1999) and can be used for nanoparticles characterization (Aslan et al. 2005). There are many studies on reflectance measurements of metal nanoparticles with different optical methods such as transmission-localized SP resonance spectroscopy (T-LSPR); propagating SP resonance spectroscopy (P-SPR); polarization-selective Fourier transform infrared reflection absorption spectroscopy (PS-FTIRRAS); polarization–modulation Fourier transform infrared reflection absorption spectroscopy (PM-FTIRRAS); surface-enhanced infrared reflection absorption spectroscopy (SEIRRAS); transmission electron microscopy (TEM); small-angle X-ray scattering (SAXS); and extended X-ray absorption and ellipsometry (Harada et al. 2009; Roy and Fendler 2004).

Despite the plethora of research done on reflectance measurements of metal nanoparticles, no studies have been performed investigating the effects of particle SD and concentration of Au, Al, and Ag nanospheres on a gold film on the angular reflectance variance. In this article, we numerically study the sensitivity of the angular reflectance to the SDs and the concentrations of single metallic nanoparticles ($10 \text{ nm} \leq d \leq 100 \text{ nm}$) on a 50-nm-thick gold film in an SP field. After discussing the fundamentals behind the SP response and briefly outlining our numerical approach, we show that it is possible to measure the particle diameters of metal nanospheres in a suspension at proper concentration levels. The detectable size limit of gold, aluminum, and silver nanospheres are also calculated to characterize the size of nanospheres based on the reflectance at different incident angles.

## Surface plasmon response

SP waves are the quanta associated with longitudinal waves propagating in matter through the collective

motion of large numbers of electrons. The wave vector of SP (see Fig. 1) can be written as

$$k_{sp}(\alpha_i, \omega) = k'_{sp} + ik''_{sp} = \left(\frac{\omega}{c}\right)\sqrt{\frac{\varepsilon_2\varepsilon_3}{(\varepsilon_2 + \varepsilon_3)}} \tag{1}$$

where, $c$ is the velocity of light and $\varepsilon$ the dielectric constant of the medium, which is a function of material properties and wavelength. The $x$-axis component of wave vector of incident light is given as

$$k_x(\alpha_i, \omega) = \sqrt{\varepsilon_1(\omega)}\left(\frac{\omega}{c}\right)\sin(\alpha_i). \tag{2}$$

The SP wave can be excited at the interface between a dielectric and conducting medium if the wave vector of the incident light, $\mathbf{k}_i$ is larger than the wave vector of the SP, $\mathbf{k}_{sp}$ (Fig. 1). The resonance condition of light with an excitation of SP waves occurs when

$$k'_{sp}(\alpha_i, \omega) = k_x(\alpha_i, \omega) \tag{3}$$

After substituting Eq. 1 and 2 into Eq. 3; we find that

$$\alpha_i = \arcsin\left[\sqrt{\frac{\varepsilon_2(\omega)\varepsilon_3(\omega)}{\varepsilon_1(\omega)(\varepsilon_2(\omega) + \varepsilon_3(\omega))}}\right]. \tag{4}$$

The SP is mainly a function of two independent parameters: the wavelength $\lambda$ (or, the frequency $\omega$) and the angle of incidence $\alpha_i$. A three-layer medium, where 1, 2, and 3 correspond to the prism, metal film, and suspension of metal particles, respectively, is shown in Fig. 1. If $\lambda$ and the total volume of medium 3 are kept constant, then the effect of the incident angle on the reflected light can be investigated for



**Fig. 1** Optical arrangement to excite SP waves

monitoring changes in the dielectric constant of medium 3.

There are two widely used configurations to excite SP: the Kretchmann–Raether configuration is the most widely used for sensor development because the volume of medium 3 (cover medium) can be adjusted unlike in the Otto configuration. Figure 1 shows the Kretchmann–Raether configuration commonly used to generate SP waves (Raether 1988). The intensity of the surface electromagnetic radiation ($I_{SP}$) has a maximum at $z = 0$, $x = 0$, and it exponentially decays along the $z$-axis normal to the interface.

The SP waves have been used extensively in the development of optical sensors for the measurement of chemical and biological components (Homola et al. 1999) and the characterization of surface and thin films (Agranovich and Mills 1982). Recently, considerable progress has been made in the systematic application of SP waves as a diagnostic tool for obtaining the characteristics of thin films, defects, and coatings (Ditlbacher et al. 2000; Lyon et al. 1998; Hutter et al. 2001). Optical properties of metal thin films can be obtained by measuring the SP response of a thin film, as demonstrated by Kolomenskii et al. (2000), who showed that the change in the absorption coefficient of different thicknesses of gold film over the visible wavelength spectrum maybe significant.

## Dielectric functions of media

If there are metallic particles such as silver or gold on the thin metallic layer as shown in Fig. 1, then the interaction of these metal particles with the surface electromagnetic radiation yields a highly dispersive dielectric constant ($\varepsilon$) at optical frequencies. In particular, the real part of the permittivity ($\varepsilon'$) changes its sign when the illumination frequency passes the threshold value (Agranovich and Mills 1982). For particles smaller than the skin depth, this microscopic interaction can result in a resonance of the entire particle, known as a plasmon resonance or a surface mode of the particle (Kreibig and Vollmer 1995). This plasma resonance can be localized in the $x$-direction (parallel to the surface) (Fig. 1) (Raether 1988). The scattered light profiles due to the presence of these small particles contain information about the particles' shape and their SDs.
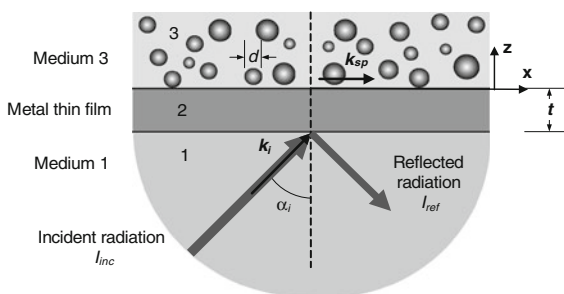
If we assume that the dielectric constant of a medium consists of real ($\varepsilon'$) and imaginary ($\varepsilon''$) parts such as $\varepsilon = \varepsilon'' + i\varepsilon''$, then the dielectric constants of media 1, 2, and 3 (shown in Fig. 1) can be written as

$$\varepsilon_1(\omega) = \varepsilon_1'(\omega) + i\varepsilon_1''(\omega), \qquad \varepsilon_1''(\omega) = 0 \qquad (5)$$

$$\varepsilon_2(\omega) = \varepsilon_2'(\omega) + i\varepsilon_2''(\omega), \qquad \varepsilon_2''(\omega) < 0 \qquad (6)$$

$$\varepsilon_{3\text{eff}}(\omega) = \varepsilon_{3\text{eff}}'(\omega) + i\varepsilon_{3\text{eff}}''(\omega) \qquad (7)$$

The dielectric constant of the prism (medium 1) is expressed as

$$\varepsilon_1(\omega) = \varepsilon_1'(\omega) = n_1^2(\omega) \qquad (8)$$

where $n_1(\omega)$ is the refractive index of the prism. The existence of a plasma resonance of the thin metal layer leads to a complex frequency $\Omega = \omega_P - i\omega_d$. Its real part corresponds to the plasma frequency of the metal film, and its imaginary part represents the damping frequency of the plasma resonance $\omega_d$. Based on this complex frequency, the real and imaginary parts of the dielectric constant of the metal layer (medium 2) and the metallic particles in the medium 3 can be obtained by the Drude model (Bohren and Huffman 1983) in the visible spectrum range as

$$\varepsilon(\omega) = \varepsilon'(\omega) + i\varepsilon''(\omega)$$
$$= \varepsilon^\infty - \frac{1}{\omega^2 + \omega_d^2}\left(\omega_p^2 - i\frac{\omega_p^2\omega_d}{\omega}\right) \qquad (9)$$

where $\varepsilon^\infty$ is the high frequency dielectric constant of the metal, $\omega_p$ is the plasma frequency, $\omega_d$ is the damping frequency, and $\omega$ is the frequency of the incident light. Experimental studies show that the data reported for most metals are in good agreement with the Drude predictions at short wavelengths.

If we assume that the medium 3 is a suspension of metallic particles and if the size of the metallic particles is small compared with the wavelength of the incident light, then the effective dielectric constant of the mixture is obtained from the Maxwell–Garnett formula (Maxwell–Garnett 1906):

$$\varepsilon_{3\text{eff}}(\omega) =$$
$$\varepsilon_s(\omega)\frac{\varepsilon_{mp}(\omega) + 2\varepsilon_s(\omega) + 2f_v\big(\varepsilon_{mp}(\omega) - \varepsilon_s(\omega)\big)}{\varepsilon_{mp}(\omega) + 2\varepsilon_s(\omega) - f_v\big(\varepsilon_{mp}(\omega) - \varepsilon_s(\omega)\big)} \qquad (10)$$

where $\varepsilon_{mp}(\omega)$ is the complex dielectric constant of the metallic particles calculated from Eq. 9, $\varepsilon_s(\omega)$ is the dielectric constant of the suspension, and $f_v$ is the total volume fraction occupied by the metallic particles. We can write the volume fraction of the spherical particles (that is, the total volume of particles per unit volume) as

$$f_v = \frac{4\pi}{3}\int_0^\infty d^3 n(d)dd \qquad (11)$$

where $d$ is the diameter of metallic particle, and $n(d)$ is its normalized SD function. The region of validity of Eq. 10 depends on the dielectric constants of the suspension $\varepsilon_s(\omega)$ and those of the metallic particles, $\varepsilon_{mp}(\omega)$. It is clear that the highest value of the volume fraction (i.e., when the same size spheres are touching each other) can be calculated from Eq. 11 as $(f_v)_{\max} = \pi/6 \approx 0.523$ (Barrera et al. 1990). For particles in suspension, it is difficult to reach this level. We will show later results for up to $f_v = 0.065$ that corresponds to $d = 50$ nm and $N_T = 1000$ particles/$\mu$m$^3$.

The effective dielectric constant of the mixture $\varepsilon_{3\text{eff}}(\omega)$ reduces to $\varepsilon_s(\omega)$ when $f_v = 0$ and $\varepsilon_{mp}(\omega)$ when $f_v = 1$. As long as all particles are spherical and there is a monodisperse mixture, it has been shown that the Maxwell–Garnett formula is an acceptable approximation to define the effective dielectric constant of the mixture (McPhedran and McKenzie 1978).

## Reflectance

Usually, the SP resonance can be excited with a P-polarized incident light because the P-polarized light produces oscillating surface electrons of a thin metallic film more easily than the S-polarized one. If a P-polarized light is incident on the surface at an angle $\alpha_i$, using the three-layer Fresnel equations, then reflectance is calculated from reflectivity equations in all the three surfaces. We then obtain total reflectance (Stratton 1941):

$$I_r(\alpha_i,\omega,t) = \frac{I_{\text{ref}}}{I_{\text{inc}}}$$
$$= \left|\frac{r_{12}(\alpha_i,\omega) + r_{23}(\alpha_i,\omega)\exp(i2k_{2z}(\alpha_i,\omega)t)}{1 + r_{12}(\alpha_i,\omega)r_{23}(\alpha_i,\omega)\exp(i2k_{2z}(\alpha_i,\omega)t)}\right|^2 \qquad (12)$$

where $r_{jl}$ is reflectivity between medium $j$ and $l$, and it can be written:

$$r_{jl}(\alpha_i, \omega) = \frac{\varepsilon_l(\omega)k_{jx}(\alpha_i) - \varepsilon_j(\omega)k_{lz}(\alpha_i)}{\varepsilon_l(\omega)k_{jx}(\alpha_i) + \varepsilon_j(\omega)k_{lz}(\alpha_i)} \qquad (13)$$
$$\text{for } j = 1, 2 \text{ and } l = 2, 3,$$

where $k_{pz}$ is the $z$-axis component of the wave number of medium $p$ .

$$k_{pz}(\alpha_i, \omega) = \sqrt{\left(\varepsilon_p(\omega)\left(\frac{\omega}{c}\right)^2 - k_x^2(\alpha_i, \omega)\right)} \qquad (14)$$
$$\text{for } p = 1, 2, 3.$$

From Eqs. 6, 9, and 10, we see that scattered light intensity is related to the effective dielectric constant of medium 3. This relation will be discussed here to determine whether we can correlate its profile with the particle size and the particle SD.

## Size distribution of nanospheres

A more accurate analysis of light scattering from particles in a medium must take into account the SD of particles within the medium. The objective of such an analysis is to determine a distribution function $f(r)$ that represents the actual SD. If we consider all sizes within the volume, then the total number of particles per unit volume can be written as

$$N_T = \int_0^\infty n(x)dx \qquad (15)$$

If we assume that the distribution can be represented by a continuous function within a given range $d_{max} \le x \le d_{min}$, then the total number of particles is obtained from

$$N_T = \int_{d_{min}}^{d_{max}} [n(x)dx] \qquad (16)$$

The SD function is normalized to unity with a diameter between $d_{min}$ and $d_{max}$:

$$\int_{d_{min}}^{d_{max}} n(x)dx = 1 \qquad (17)$$

where $n(x)$ is the normalized SD function.

There are several distribution functions for particle SDs that cover a wide range of SD possibilities.

Distributions encountered in real applications are generally non-Gaussian, because the particles face more extreme conditions (temperature, pressure, forces, etc.) during their synthesis (/fabrication) than those expected for a Gaussian distribution. However, a distribution that is normal in the logarithm of a parameter often provides a reasonable fit to observations. Another advantage of the log-normal distribution is that it is positive-definite, so it is often useful for representing quantities that cannot have negative values. Here we consider only a log-normal distribution which has been employed widely in light scattering studies (Kerker 1969). A log-normal distribution has proven useful for representing the SDs of all kinds of small particles and aerosols. The general form of a log-normal distribution that we consider here is (Hansen and Travis 1974):

$$n(d) = \sqrt{\frac{2}{\pi}}\frac{1}{\sigma_g d}\exp\left\{-\left[\ln(d/2) - \ln(D_g/2)\right]^2 \Big/ \left(2\sigma_g^2\right)\right\} \qquad (18)$$

where $\sigma_g$ is variance distribution, and $D_g$ is the characteristic diameter. Effective diameter $d_{eff}$ and the effective variance $v_{eff}$ are related by

$$v_{eff} = \frac{\int_0^\infty (d - d_{eff})^2 d^2 n(d)dd}{\int_0^\infty d_{eff}^2 d^2 n(d)dd} \qquad (19)$$

and may be expressed as

$$d_{eff} = D_g \exp\left(5\sigma_g^2\Big/2\right) \text{ and } v_{eff} = \exp\left(\sigma_g^2\right) - 1 \qquad (20)$$

.

In this study, the SD of metallic nanospheres is described in terms of an effective diameter $d_{eff}$ and an effective variance $v_{eff}$. Figure 2 shows the dependence of the log-normal SD function on the effective diameter and effective variance. We can say that the shape of the log-normal SD strongly depends on the values of $d_{eff}$. The effective variance $v_{eff}$ does not affect the SD especially for small values of effective variance which makes the SD a little narrower. Therefore, in this study, we assume that $d_{eff}$ is the only parameter that strongly affects the SD; $v_{eff}$ is assumed constant ($v_{eff} = 0.1$).
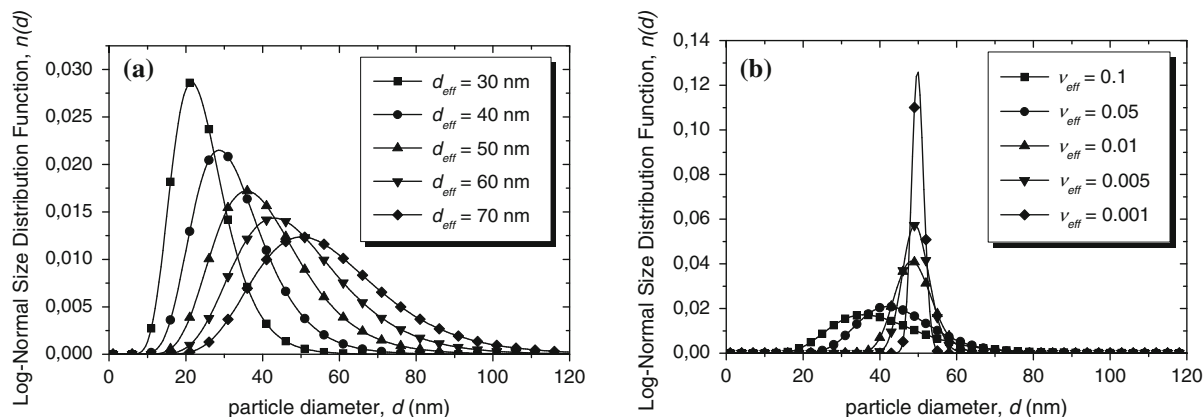
**Fig. 2** Log-normal SD parameters: **a** Effective diameter $d_{eff}$ for $v_{eff} = 0.1$, and **b** effective variance, $v_{eff}$ for $d_{eff} = 50$ nm

## Numerical procedure

Numerical calculations were carried out using a code developed in MATLAB 6.1. Numerical data for the reflectance ($I_r$) were calculated as a function of the incident angle ($\alpha_i$), and the metallic volume fractions ($f_v$) of nanoparticles as well as particle effective diameter ($d$) using Fresnel optics were calculated by the MATLAB code. The input parameters were the optical properties of the three media: wavelength $\lambda$, thickness of metallic thin film $t$, maximum $d_{max}$, minimum $d_{min}$, effective particle diameter $d_{eff}$, number of particles per unit volume $N_T$ and incident angle $\alpha_i$.

The first medium considered was sapphire with a refractive index of $m_1 = 1.79 + i\,0.0$ at $\lambda = 632$ nm. The second medium (metallic thin film) was gold with optical properties as listed in Table 1 (Bass 1995; Modest 1993). The third medium consisted of metallic nanospheres suspended in ethanol, which has a refractive index of $m_s = 1.36 + i0.0$ at $\lambda = 632$ nm. The most common metal nanoparticles for SP studies such as gold (Au), aluminum (Al), and silver (Ag) are chosen and the optical properties of the metals are obtained from literature (Bass 1995; Modest 1993). Table 1 gives the Drude model parameters of gold, silver, and aluminum which can be used to obtain the

**Table 1** Drude model parameters of gold, aluminum, and silver at $\lambda = 632$ nm

| Parameter Metal | $\varepsilon^\infty$ | $\omega_p$ (Hz) $\times 10^{15}$ | $\omega_d$ (Hz) $\times 10^{12}$ |
| --- | --- | --- | --- |
| Gold (Au) | 9.75 | 13.6 | 145 |
| Aluminum (Al) | 1.00 | 3.07 | 31.2 |
| Silver (Ag) | 3.40 | 2.2 | 4.3 |

refractive index values. Note that $\varepsilon^\infty$ is the high frequency dielectric constant of the metal, $\omega_p$ is the plasma frequency (Hz), and $\omega_d$ is the damping frequency (Hz).

## Results and discussion

The potential for sensing metallic nanospheres located on a thin metallic thin film based on reflectance measurements is examined by comparing numerical simulations and calculations for gold, aluminum, and silver particles on a gold thin film in the suspension. It is assumed that there is a monodisperse log-normal SD, that the particles are spherical in shape, and that surface of the thin film is very smooth.

### Angular dependency of reflectance

The reflectance of three different metal particles (gold, aluminum, and silver) was calculated based on the optical properties obtained from Eq. 9, where it is assumed that the particles are suspended in ethanol on a 50-nm-thick gold film. For different particle volume fractions ($f_v$'s), the reflectance was calculated and plotted in Fig. 3. It is obvious that the reflectance is very sensitive to the particle volume fraction for some special incident angles. Even though the Maxwell–Garnett mixing formula (Eq. 6) is assumed to be valid only for a small volume fraction ($f_v \ll 1$) (Doyle 1978), in general, it is acceptable even for high particle volume fractions if we assume that
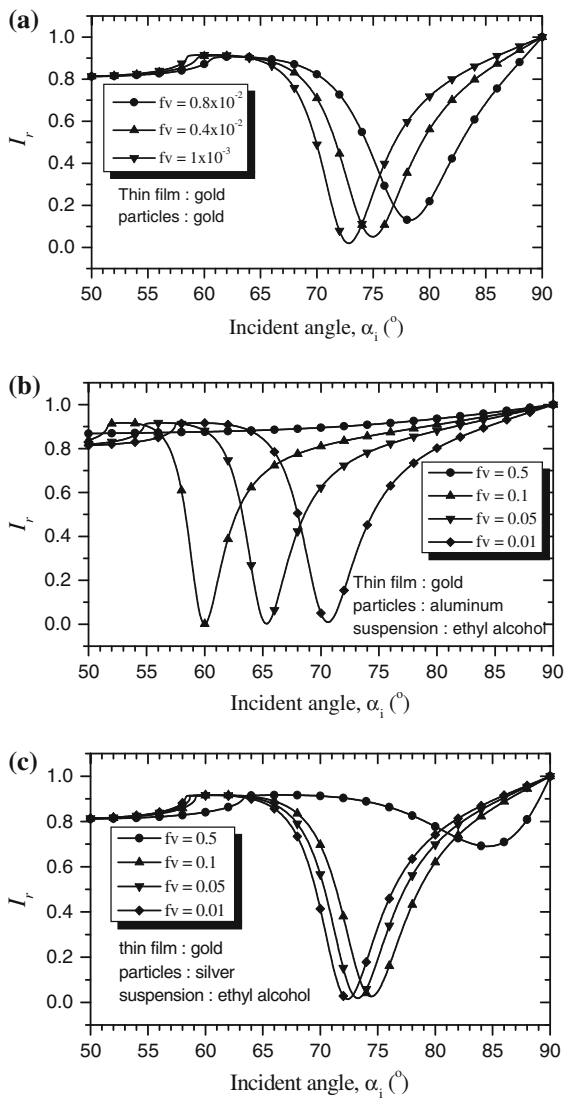
**Fig. 3** Reflectance as a function of incident angle, and different metallic particles in ethanol; **a** gold, **b** aluminum, and **c** silver

particles are spheres and are uniformly distributed in the suspension. The minimum reflectance shifts as a function of the volume fraction as well as with material type of the nanospheres. For gold particles at small volume fractions ($f_v < 0.01$), the shift of the incident angle for minimum reflectance is significant.

Effect of particle diameter on reflectance

In order to understand the effect of the particle diameter clearly, the number of particles in a unit volume $N_T$ is varied from 10 to 1000 particles/μm³,

and three different monodisperse SDs are assumed: uniform size particles ($d_{eff} = d_{max} = d_{min}$), a narrow SD ($0.7d_{eff} \leq d \leq 1.3d_{eff}$), and a broad SD ($0.2d_{eff} \leq d \leq 1.8d_{eff}$). The effective variance is kept constant ($v_{eff} = 0.1$) for the calculations. Figures 4, 5, and 6 show how the angular reflectance is sensitive to the particle sizes for the Ag, Al, and Au nanospheres with three different $N_T$ (10, 100, and 1000 particles/μm³) and SD. In the figures, the rows represent constant $N_T$, and the columns represent the SDs. Effective particle diameter was kept constant as $v_{eff} = 0.1$ for all calculations shown in Figs. 4, 5, and 6. Figure 4 shows that if the particles are of gold on a gold thin film, then detection of particle effective diameter of gold spheres in the ethanol suspension is possible with high sensitivity. The range of detectible effective diameters of silver particles is from 10 nm up to 110 nm depending on the value of $v_{eff}$. In Fig. 4, the numbers of particles per unit volume are 10, 100, and 1000 in each row. The effective silver particle size with a SD can be detectable in the medium particle volume fraction. If the particles are gold on a 50-nm-thick gold film, then it can be said that regardless of $v_{eff}$ and the width of the SD, the reflectance at $\alpha_i = 72°/80°$ is very sensitive to particles whose diameter is between 10 nm and 70 nm. The 2D reflectance graph for aluminum spheres on gold thin film shown in Fig. 5 is different from the results for silver particles shown in Fig. 4. If the particle volume fraction is higher ($N_T > 100$ particles/μm³), then the particle size can be detected. When the particle volume fraction of aluminum nanospheres is higher, sensitivity to size is higher for the smaller aluminum nanospheres. The results from gold particles on a gold film are shown in Fig. 6. When $N_T > 100$ particles/μm³, it is possible to detect gold particles with a wide SD. In this case, the reflectance is very sensitive to the particle with effective diameter up to 70 nm, and still particles with effective diameters between 70 nm and 110 nm can be detected with reduced sensitivity.

**Conclusion**

In this study, reflectance ($I_r$'s) of gold, silver, and aluminum nanospheres dispersed in ethanol on a thin gold film were mapped as a function of both the incident angle and effective diameter of the
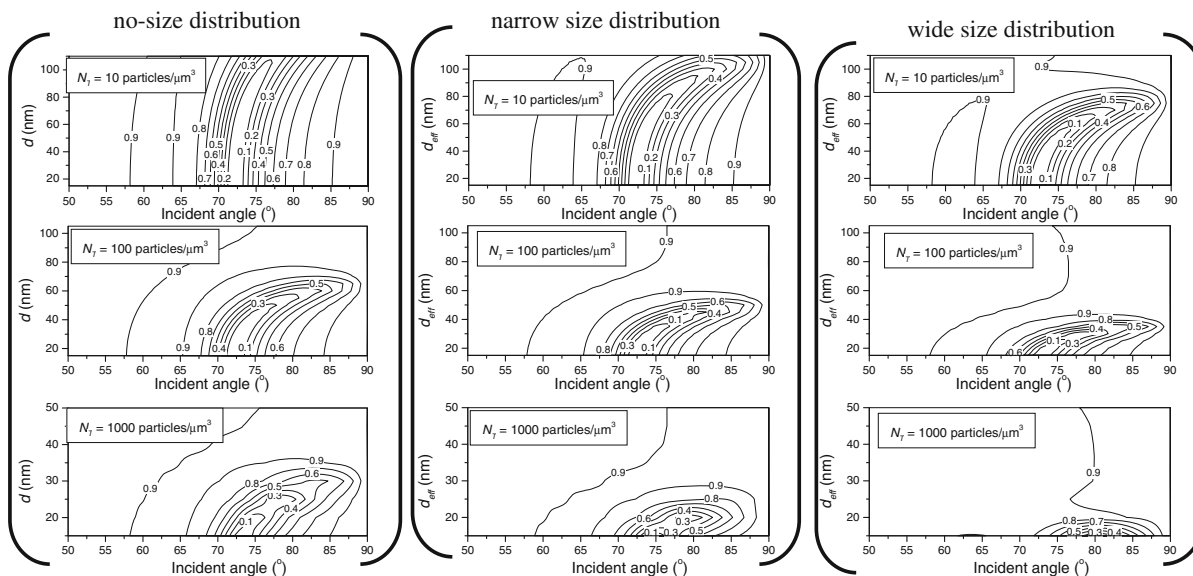
no-size distribution    narrow size distribution    wide size distribution



**Fig. 4** Reflectance for gold (Au) spheres on the gold film (strong SP resonance zone if reflectance <0.1)

no-size distribution    narrow size distribution    wide size distribution
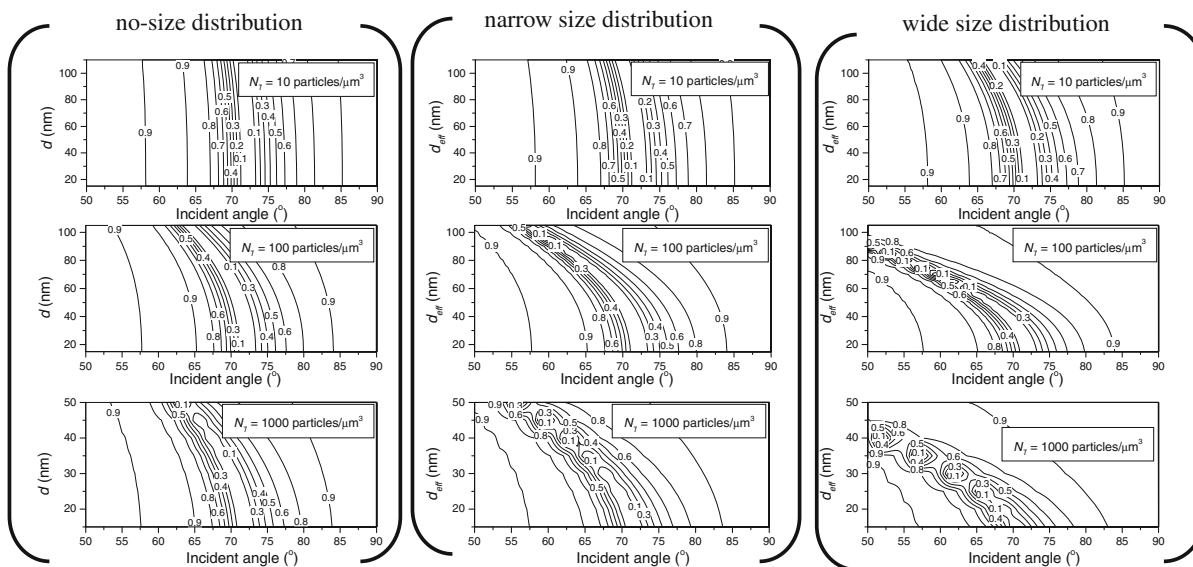


**Fig. 5** Reflectance for aluminum (Al) spheres on the gold film (strong SP resonance zone if reflectance <0.1)

nanospheres as shown in Figs. 4–6. At low volume fractions, reflected light does not indicate any significant variation by altering the average sphere diameter for all the three types of metals. With a higher number of particles per unit volume, it is evident that the reflectance maps show a dependence on the effective size of Ag, Al, and Au metallic nanospheres

($d_{eff}$ <100 nm), but the sensitivity of the dependency varies depending on the metal. The optimum incident angle to detect the size of nanospheres with a SD can be chosen between 70° and 75° for a given volume fraction of particles. The degree of sensitivity of the reflectance on the diameter of spherical metal nanoparticle $d$ depends on the optical properties on both
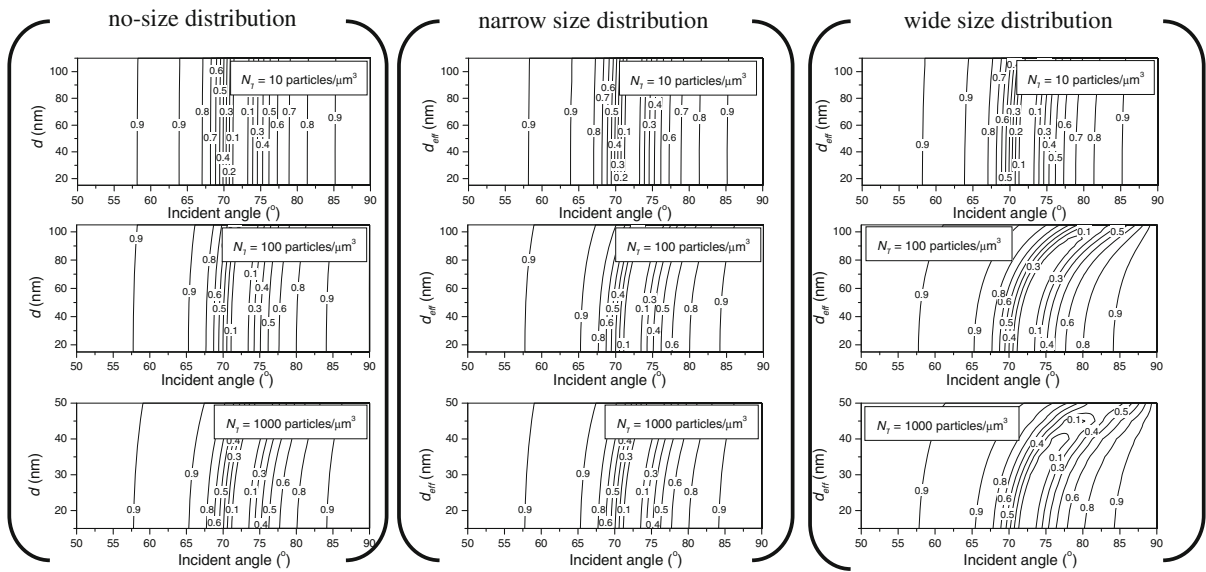
**Fig. 6** Reflectance for silver (Ag) spheres on the gold film (strong SP resonance zone if reflectance <0.1)

the thin film and the nanospheres. A high number of particles per unit volume with a wider SD make the incident angle more sensitive to the effective diameter of the nanospheres.

This numerical study shows that SP-wave-reflected light phenomena can be used to characterize metal nanospheres with a SD in suspension on a gold film. In general, particles with diameters up to 100 nm can be detected using this method. The effective particle diameter $d_{eff}$ of metallic nanospheres with a SD can be obtained if the appropriate particle volume fraction is chosen for the incident light angle. In particular, the optimum incident angle needed to relate the diameter of particles to the reflected light can differ from one type of metallic particle to another. Taking into account the size effect for nanoparticles would result in more accurate calculation of the dielectric constants for nanospheres (Scaffardi and Tocho 2006). In this study, results are given for one wavelength (632 nm) only, but it is well known that SP resonance peak points of gold, aluminum, and silver shift depending on the size of the nanospheres. Therefore, there is a need to explore other wavelengths that are sensitive to the size at a given $N_T$ to fully map the spectral dimension of the reflectance. Future experimental reflectance measurements of the metal nanoparticles with SDs will be conducted to meet this need.

## References

Agranovich VM, Mills DL (1982) Surface Polaritons. North-Holland Pub Co, Amsterdam

Aslan MM, Videen G, Menguc MP (2005) Characterization of metallic nano-particles via surface wave scattering: B. physical concept numerical framework. J Quant Spectrosc Radiat Transf 93:207–217. doi:10.1016/j.jqsrt.2004.08.040

Barrera RG, Villasenor–Gonzalez P, Mochan WL, Monsivais G (1990) Effective dielectric response of polydispersed composites. Phys Rev B 41:7370–7376

Bass M (1995) Handbook of optics. McGraw-Hill, New York

Berne BJ, Pecora R (1976) Dynamic light scattering. Wiley, New York

Bohren CF, Huffman DR (1983) Absorption and scattering of light by small particles. Wiley, New York

Brune H, Giovannini M, Bromann K, Kern K (1998) Self-organized growth of nanostructure arrays on strain-relief patterns. Nature 394:451–453. doi:10.1038/28804

Ditlbacher H, Krenn JR, Lamprecht B, Leitner A, Aussenegg FR (2000) Spectrally coded optical data storage by metal nanoparticles. Opt Lett 25(8):563–565. doi:10.1364/OL.25.000563

Doyle WT (1978) The Clausius-Mossotti problem for cubic arrays of spheres. J Appl Phys 49:795–797. doi:10.1063/1.324659

Feldheim DL, Foss CA (2002) Metal nanoparticles : synthesis, characterization, and application. Marcel Dekker Inc, New York

Hansen JE, Travis LD (1974) Light scattering in planetary atmospheres. Space Sci Rev 16:527–610

Harada M, Saijo K, Sakamoto N (2009) Characterization of metal nanoparticles prepared by photoreduction in aqueous solutions of various surfactants using UV-vis, EXAFS and SAXS. Colloids Surf A-Physicochem

Eng Aspects 349:176–188. doi:10.1016/j.colsurfa.2009.08.015

Homola J, Yee SS, Gauglitz G (1999) Surface plasmon resonance sensors: review. Sens Actuators B-Chem 54:3–15

Hutter E, Fendler JH (2004) Exploitation of localized surface plasmon resonance. Adv Mater 16:1685–1706. doi:10.1002/adma.200400271

Hutter E, Fendler JH, Roy D (2001) Surface plasmon resonance studies of gold and silver nanoparticles linked to gold and silver substrates by 2-aminoethanethiol and 1, 6-hexanedithiol. J Phys Chem B 105:11159–11168. doi:10.1021/jp011424y

Kerker M (1969) The Scattering of light and other electromagnetic radiation. Academic Press, New York

Kolomenskii AA, Gershon PD, Schuessler HA (2000) Surface-plasmon resonance spectrometry and characterization of absorbing liquids. Appl Opt 39:3314–3320. doi:10.1364/AO.39.003314

Kreibig U, Vollmer M (1995) Optical properties of metal clusters. Springer Verlag, New York

Kruis FE, Fissan H, Peled A (1998) Synthesis of nanoparticles in the gas phase for electronic, optical and magnetic applications—A review. J Aerosol Sci 29:511–535. doi:10.1016/S0021-8502(97)10032-5

Lyon LA, Musick MD, Natan MJ (1998) Colloidal Au-enhanced surface plasmon resonance immunosensing. Anal Chem 70:5177–5183. doi:10.1021/ac9809940

Lyon LA, Pena DJ, Natan MJ (1999) Surface plasmon resonance of Au colloid-modified Au films: particle size dependence. J Phys Chem B 103:5826–5831. doi:10.1021/jp984739v

Maxwell-Garnett JC (1906) Colours in metal glasses, in metallic films, and in metallic solutions II. Philos Trans R Soc Lond Ser A 205:237–288

McPhedran RC, McKenzie DR (1978) The conductivity of lattices of spheres. I. the simple cubic lattice. Proc R Soc Lond Ser A 359:45–63

Modest MF (1993) Radiative heat transfer. McGraw-hill Inc, New York

Raether H (1988) Surface plasmons on smooth and rough surfaces and on gratings. Springer-Verlag, Berlin

Roy D, Fendler J (2004) Reflection and absorption techniques for optical characterization of chemically assembled nanomaterials. Adv Mater 16:479–508. doi:10.1002/adma.200306195

Scaffardi R, Tocho J (2006) Size dependence of refractive index of gold nanoparticles. Nanotechnology 17:1309–1315. doi:10.1088/0957-4484/17/5/024

Shipway AN, Katz E, Willner I (2000) Nanoparticle arrays on surfaces for electronic, optical, and sensor applications. ChemPhysChem 1:18–52. doi:10.1002/1439-7641(20000804)1:1<18:AID-CPHC18>3.0.CO;2-L

Stratton JA (1941) Electromagnetic Theory. McGraw-Hill, New York

Wriedt T (2009) Light scattering theories and computer codes. J Quant Spectrosc Radiat Transf 110:833–843. doi:10.1016/j.jqsrt.2009.02.023